Colloids and Surfaces A: Physicochemical and Engineering Aspects 703 (2024) 135207

Contents lists available at ScienceDirect

Colloids and Surfaces A: Physicochemical and Engineering Aspects

journal homepage: www.elsevier.com/locate/colsurfa

Strategically engineered multifunctional graphene oxide hybrid nanomaterials for efficient catalytic degradation and emerging contaminants treatment

Ghizlane Achagri [a,b], Othmane Dardari [c,d], Othmane Amadine [d], Abudukeremu Kadier [a,b,*], Younes Essamlali [d], Ghita Radi Benjelloun [e], Mohamed Zahouily [c,d,**], Farooq Sher [f,***]

[a] Laboratory of Environmental Science and Technology, The Xinjiang Technical Institute of Physics and Chemistry, Key Laboratory of Functional Materials and Devices for Special Environments, Chinese Academy of Sciences, Urumqi 830011, China
[b] Center of Materials Science and Optoelectronics Engineering, University of Chinese Academy of Sciences, Beijing 100049, China
[c] Laboratory of Materials, Catalysis and Valorization of Natural Resources. Hassan II University, Casablanca, FST-Mohammedia, B.P. 146, 20650, Morocco
[d] Moroccan Foundation for Advanced Sciences, Innovation and Research (MASCIR Foundation), Rabat Design, Rue Mohamed El Jazouli, Madinat El Irfane, Rabat 10100, Morocco
[e] Laboratoire de Biochimie, Environnement et Agroalimentaire, University of Hassan II Casablanca, Faculty of Sciences and Technologies Mohammedia, Morocco
[f] Department of Engineering, School of Science and Technology, Nottingham Trent University, Nottingham NG11 8NS, United Kingdom

HIGHLIGHTS

- A Novel multifunctional $CoFe_2O_4$/GO hybrid nanomaterial-coated PET fabric was successfully obtained.
- The prepared fabric exhibited improved thermal stability and mechanical properties with high catalytic performance.
- $CoFe_2O_4$/GO synergistically endows the fabric with antibacterial activity against *S.aureus* and *E.coli bacteria*.
- The PET/ $CoFe_2O_4$/GO fabric showed excellent catalytic performance for peroxymonosulfate activation in Rhodamine B degradation reaction.

GRAPHICAL ABSTRACT

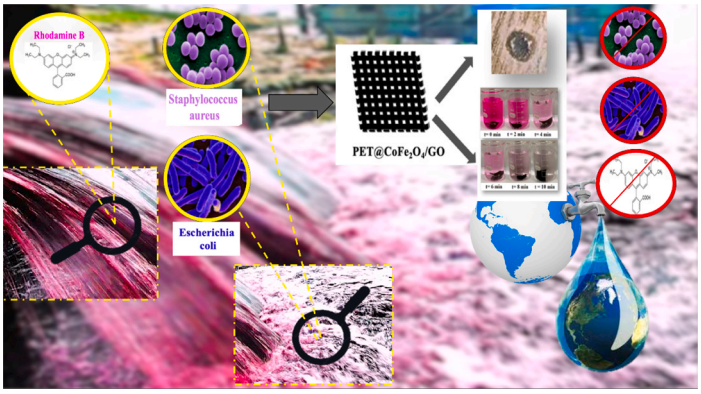

ARTICLE INFO

Keywords:
Pollution
Polyester (PET) fabric

ABSTRACT

The use of functional textiles is growing in all fields of science and technology. Surface functionalization is mainly used to impart conventional textiles with new functionalities and improved performances. In the present study, a cobalt ferrite nanoparticle/graphene oxide ($CoFe_2O_4$/GO) coated polyethylene terephthalate (PET)

* Corresponding author at: Laboratory of Environmental Science and Technology, The Xinjiang Technical Institute of Physics and Chemistry, Key Laboratory of Functional Materials and Devices for Special Environments, Chinese Academy of Sciences, Urumqi 830011, China.
** Corresponding author at: Laboratory of Materials, Catalysis and Valorization of Natural Resources. Hassan II University, Casablanca, FST-Mohammedia, B.P. 146, 20650, Morocco.
*** Corresponding author.
E-mail addresses: abudukeremu@ms.xjb.ac.cn (A. Kadier), m.zahouily@mascir.com (M. Zahouily), Farooq.Sher@ntu.ac.uk (F. Sher).

https://doi.org/10.1016/j.colsurfa.2024.135207
Received 29 January 2024; Received in revised form 10 August 2024; Accepted 26 August 2024
Available online 28 August 2024

Surface functionalization
Nanotechnology
RhB degradation
Catalytic performance

fabric with excellent catalytic and antibacterial properties, has been successfully developed. The PET-coated $CoFe_2O_4$/GO samples, ranging from 1 % to 5 % wt. were obtained using a simple dip-coating method in CoFeO/GO solution (1 mg/mL), and were investigated through several physiochemical characterization techniques. $CoFe_2O_4$/GO and PET fabric have been shown to establish an interfacial connection by Fourier transform infrared spectroscopy (FTIR). X-ray diffraction (XRD) results showed that $CoFe_2O_4$/GO coating did not affect the PET crystallinity and that $CoFe_2O_4$/GO hybrid was incorporated in the PET samples, which was proved as well by the morphological study through Scanning electron microscopy (SEM). Furthermore, thermogravimetric characterisation (TGA) verified that the coating does not change or impair the quality of the fibre and that the PET@$CoFe_2O_4$/GO as made is thermally stable. Tensile strength tests demonstrated that coated fabrics exhibited outstanding mechanical properties in comparison with pristine PET. Moreover, the coated PET@$CoFe_2O_4$/GO fabric was used as a model catalytic system for peroxymonosulfate (PMS) activation in the rhodamine B (RhB) degradation reaction. Total Organic Carbon (TOC) measurements showed that TOC removal reached 89.82 % in only 12 min reaction. The results confirmed that the coated fabrics exhibited high catalytic performances, good stability and reusability in consecutive degradation experiments with a degradation rate over 60 % even after 7 degradation cycles; Moreover, it is easily and simply separated from the mixture, by removing the textile sample from the aqueous solution. It is worth mentioning that the PET@$CoFe_2O_4$/GO fabrics showed outstanding antibacterial activity against both *Staphylococcus aureus* (Gram-positive) and *Escherichia coli* (Gram-negative) bacteria with an inhibition diameter zone of up to 13 mm for PET@$CoFe_2O_4$/GO (5 %). Overall, these findings are of great importance as they permit the development of a novel multifunctional textile fabric, combining antibacterial activity, catalytic performance and mechanical properties. The study provides a textile-based catalyst with improved catalytic performance, re-usability in consecutive degradation reactions and easy catalyst separation compared to traditional supports. Thus, a huge potential application in several fields such as medicine, heterogeneous catalysis, and wastewater treatment.

1. Introduction

Currently, developing textile materials with high technical properties is of great interest. Multifunctional textiles are used for various applications such as engineering, packaging, comfort, medicine, clothing, protection, catalysis and others [1,2]. Thus, the development of functional textiles allows the introduction of new interesting and original functionalities, either through working on the fibre's architecture [3] or via surface modification [4]. Therefore, the challenge is to bring new features that are ecological and transferable to the industrial scale. In addition, the mechanical flexibility, low cost and lightweight properties of multifunctional textiles have rendered these materials an ideal choice for several applications. Recently, numerous studies have reported modulating textile materials' properties by the incorporation of nanometric fillers. Metallic nanoparticles [5], carbon nanotubes (CNT) [6], silver nanoparticles [7] and graphene [8] are among the most used nano-fillers for textile modification. It's interesting to note that because of their exceptional flexibility, superior thermal and chemical stability, and chemical modification potential, graphene and its derivatives have attracted a lot of attention [9]. Incorporating small weight percentages of nanofillers in the textile matrices endows them with excellent properties, which are closely related to the percentage of these nanofillers in textile matrices. However, textile fabric functionalization is to be utilized in different applications. Most of the functionalization methods, including sol-gel-based coating, wet chemical process, and electro-deposition, present limitations, either in the complex manufacturing process or the hard transfer into large-scale applications. In this regard, the dip-coating technique is recognized as a promising approach due to its easy processing and applicability for large-scale applications [10].

In recent years, the rapid growth of technological and industrial technologies has led to increasing utilization of organic matter. As a consequence, a dramatic increase in environmental pollution [11,12]. Water pollution is considered to be one of the most threatening problems among all of them, it has reached an alarming degree in many countries and extends worldwide [13]. Several water resources, besides being polluted by dangerous chemicals, are also contaminated by pathogenic microorganisms. The presence of bacteria in drinking water, specifically E.*coli,* may cause harmful consequences such as diarrhea, vomiting, cramps, fever and sometimes death. The growth in the demand for clean water accompanied by a possible shortage of drinking water is a primary concern and has attracted increasing attention [14]. Huge efforts have been devoted and several studies have aimed to find efficient and ecological wastewater treatment to remedy this problem [15,16].

Cobalt ions (Co) are one of the common transition metallic ions utilized in catalytic decomposition reactions [17]. An encouraging way to remove various pollutants from wastewater would be to use co-based catalysts, such as organic molecules and heavy metals [18]. Recently, Wu et al. [19] used cobalt (II,III) oxide (Co_3O_4) for the activation of peracetic acid (PAA) and attained high efficiency in terms of degradation of micro-organic pollutants. Jing Di and his co-workers [20] investigated the utilization of a heterogeneous Co-based catalyst for Rhodamine B (RhB) degradation. The elaborated Co_3O_4-rice husk exhibited relevant catalytic activity during PMS activation, consequently degrading RhB in water.

Cobalt ferrites ($CoFe_2O_4$) magnetic nanoparticles are one of the most studied co-based catalysts [21]. Their outstanding properties, including large surface area, chemical stability, high antibacterial and catalytic activity, offer diverse applications in various fields [22]. In fact, $CoFe_2O_4$ magnetic nanoparticles demonstrate considerable antibacterial activities. Gheidari et al. [23] recently ex-animated the antibacterial property of $CoFe_2O_4$. The prepared materials demonstrated an antibacterial activity against different types of bacteria, such as *Staphylococcus aureus, Escherichia coli, Pseudomonas aeruginosa and Bacillus cereus*. Moreover, magnetic $CoFe_2O_4$ nanoparticles demonstrated high catalytic efficiency for the activation of peroxymonosulfate (PMS) [24,25]. On this basis, our previous study [26] reported the activation of PMS with the aim of the degradation of RhB using the magnetic catalyst cobalt ferrite nanoparticle/graphene oxide ($CoFe_2O_4$/GO). The synthesized Co-based catalysts revealed potential ability for catalytic decomposition of RhB utilizing PMS as an oxidant and exhibited stability and reusability. Although previous studies demonstrated the successful elaboration of $CoFe_2O_4$ catalyst for the degradation of RhB, most of them present several drawbacks related to the $CoFe_2O_4$ catalyst separation, which requires the employment of an external magnetic force, thus limiting their utilization for large-scale applications.

Up to date, there are no reported studies about $CoFe_2O_4$/GO catalyst as a hybrid coating on textiles for both, dye degradation and antibacterial activity. In the present work, the immobilization of the previously synthesized $CoFe_2O_4$/GO in our previous study onto PET fabrics are investigated, to develop a new class of multifunctional textiles, that combine, catalytic performances and antibacterial activity. The antibacterial characterization was performed against *Staphylococcus aureus* (Gram-positive) and *Escherichia coli* (Gram-negative) bacteria.

Moreover, since $CoFe_2O_4$/GO exhibited high catalytic performances, the coated PET@$CoFe_2O_4$/GO fabric was used as a catalytic support for the decomposition of RhB via the activation of PMS with reference to the main optimum factors of the removal of RhB in the system and results from our previous study. In addition, the incorporation of $CoFe_2O_4$/GO onto textile fabrics facilitates the catalyst separation process from the final solution, which is the main challenge for all types of catalysts, by simply removing the fabric from the solution and without the necessity of applying traditional separation techniques, such as centrifugation, filtration or magnetic separation, which is suitable for large-scale applications. The obtained outcomes hold significant value for the functionalisation, design, and fabrication of innovative multifunctional textiles possessing exceptional catalytic activity and antibacterial properties. Moreover, this study reported a new, efficient, reusable and easy method to separate catalysts, which paves the way for future researches aiming to develop textile-based catalytic supports.

2. Materials and methods

2.1. Chemicals

Pristine Polyester (PET) fabric (100 g/m^2) was purchased as a substrate. Natural graphite (purity: 99.99 %) was processed from Sigma Aldrich. All the other chemicals including sulfuric acid (H_2SO_4), permanganate ($KMnO_4$), sodium nitrate ($NaNO_3$), hydrogen peroxide (H_2O_2,), potassium, Ethanol (C_2H_6O), sodium hydroxide (NaOH), Rhodamine B ($C_{28}H_{31}ClN_2O$), peroxymonosulfate ($KHSO_5$), cobalt chloride hexahydrate ($CoCl_2$.6 H_2O) and iron chloride hexahydrate ($FeCl_3$.6 H_2O) were provided by Sigma-Aldrich.

2.2. Preparation of graphene oxide and cobalt-ferrites

The synthesis of Graphene oxide (GO) from natural graphite was achieved following Hummer's method [27] and the cobalt-ferrites/GO ($CoFe_2O_4$/GO) nanoparticles were synthesized using the co-precipitation method [28]. Briefly, graphite GO (0.16 g) was completely dispersed for 30 min in distilled water to get the brown GO solution. Independently, $CoCl_2$.6 H_2O (1.19 g) and $FeCl_3$.6 H_2O (2.7 g) were dissolved in 10 mL distilled water. The mixture was then added to GO suspension and put under stirring for 1 h. 25 mL of 12 % w/v NaOH aqueous solution was then added dropwise to the prepared dispersion while maintaining vigorous stirring. The final solution was heated at 100 °C for 1 h in a sand bath. Finally, the obtained precipitate was magnetically separated, washed until neutral pH and dried for 24 h.

2.3. Preparation of cobalt-ferrites/graphene oxide-coated fabric

The pristine PET samples (10× 4 cm) were firstly cut and pre-treated with ammonia and nonionic detergent solution for 1 h at 100 °C, then cleaned with distilled water and put to dry for 4 h at 90 °C. The coated PET@$CoFe_2O_4$/GO samples have been developed utilizing "dip-coating" methodology [29]. The pre-treated samples were dipped in $CoFe_2O_4$/GO solution (1 mg/mL) for 1 min and then dried at 90 °C for 2 h. After each cycle, the coated PET@$CoFe_2O_4$/GO sample was weighted and the loading of $CoFe_2O_4$/GO on the PET was calculated. This operation was performed repeatedly to increase the loading of $CoFe_2O_4$/GO on the PET fabrics until obtaining the desired PET@$CoFe_2O_4$/GO(1 %), PET@$CoFe_2O_4$/GO(3 %) and PET@$CoFe_2O_4$/GO(5 %) samples. During this step, the $CoFe_2O_4$/GO hybrid was uniformly coated on the surface of PET fabric. A noticeable colour variation from white to dark grey was noticed as the coting cycles increased that is observed from the digital images of PET, and all coated samples (Fig. 1).

2.4. Characterizations

The full characterizations of GO, $CoFe_2O_4$ and $CoFe_2O_4$/GO samples were described in detail in our recent related study[30]. The chemical structure and properties of the developed PET fabrics were studied using FTIR spectroscopy with an Affinity-1S spectrometer (SHIMADZU Co., Ltd., China). XRD characterization was executed on a diffractometer (Bruker D8, Germany). The colour changes of the obtained fabrics were measured by colour coordinates (L*(lightness), a* (redness-greenness), b* (yellowness-blueness)) by mean of a colour spectrophotometer BYK (spectral range: 400–700 nm). The surface morphology of PET@$CoFe_2O_4$/GO was visualized using Scanning Electron Microscopy (SEM), using an FEI Quanta 200-ESEM (SHIMADZU Co., Ltd., China). Using a thermogravimetric analysis (TGA) TGA-Q500 (TA instruments) at a heating rate of 10 °C/min in an air atmosphere between 25 °C and 600 °C, the thermal stability of all materials was investigated. The tensile properties of the PET and PET@$CoFe_2O_4$/GO fabrics were determined at a tensile speed of 10 mm/min (Shimadzu EZ-SX apparatus, China). Measurements were carried out on rectangular shapes specimens of 10 mm length, 40 mm width and 0.4 mm thickness. Total organic carbon (TOC) was studied by the Total Organic Analyzer system (Shimadzu TOC-L Series, China).

2.5. Catalytic test procedure

The catalytic performances of PET@$CoFe_2O_4$/GO were investigated based on the optimum results obtained from our previous work [26]. RhB catalytic degradation test using PET@$CoFe_2O_4$/GO(5 %) was performed using 50 mL of RhB solution (0.03 mmol/L). Briefly, 0.005 g of

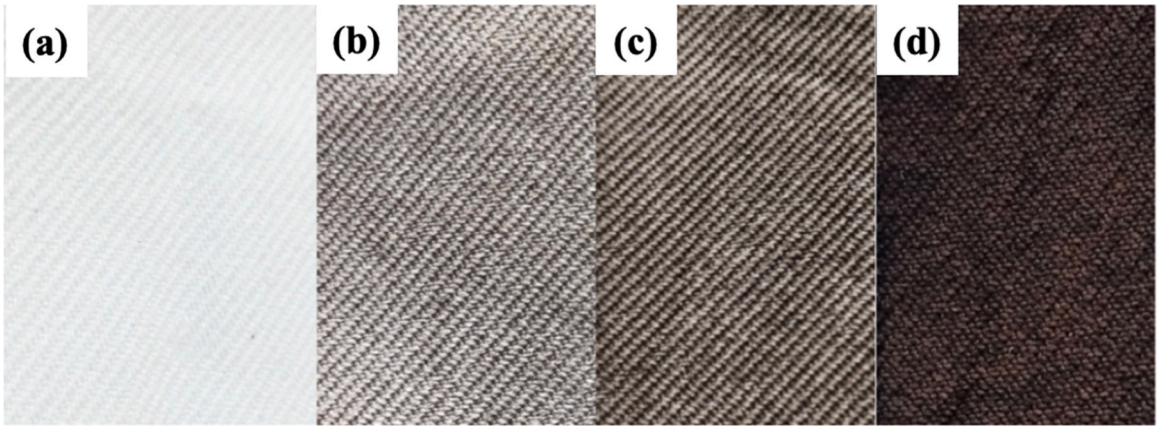

Fig. 1. Digital images of the PET samples; (a) Pristine PET, (b) PET@$CoFe_2O_4$/GO (1 %), (c) PET@$CoFe_2O_4$/GO (3 %) and (d) PET@$CoFe_2O_4$/GO (5 %).

PMS was initially added to RhB solution while stirring, afterwards, a piece of PET@$CoFe_2O_4$/GO fabric equivalent to the used mass (0.01 g of $CoFe_2O_4$/GO catalyst) was put in the solution to start the experiment, during which, RhB concentrations were calculated and determined via monitoring the decrease in the absorbance with UV–vis spectroscopy at 554 nm maximum wavelength, where A_0 and A represent the initial and final absorbance of RhB at 554 nm, and C_0 and C represent the initial and ultimate concentrations of RhB respectively. Under identical circumstances, total organic carbon (TOC) was calculated as a function of time to examine the breakdown of RhB and the mineralisation of organic species. The degradation efficiency was quantified following Eq. (1) [30].

$$\text{Degradation}(\%) = \frac{(C_0 - C) \times 100}{C_0} = \frac{(A_0 - A) \times 100}{A_0} \quad (1)$$

2.6. Biological activities

The antibacterial performance of the PET@$CoFe_2O_4$/GO textiles was investigated against *Staphylococcus aureus* (ATCC 25922, Gram-positive bacterium) and *Escherichia coli* (ATCC 25923, Gram-negative bacterium). The test was performed using disk diffusion method [31]. Circular samples of pristine PET and coated ones were prepared and autoclaved with all the glassware used at 120 °C for 20 min before use and the whole experiment was performed under sterile conditions. Mueller Hinton agar was carefully covered with bacterial suspensions before the prepared samples and the clean sample—which was selected as a reference—were added to the Petri dishes. The inhibitory zone diameters were assessed after these last were cultured for 24 hours at 37 °C.

3. Results and discussion

3.1. Structural analysis

FTIR analysis was used to verify the functionalization of different samples and to highlight the interactions established between the $CoFe_2O_4$/GO and the macromolecular chains of PET fabric. The FTIR spectra of pristine fabric as well as different loaded samples are shown in Fig. 2. The pristine sample showed the characteristic bands of PET fabric, including the bands located at 970 and 1018 cm^{-1} assigned to the C-O stretching of glycol and benzene in-plane vibrations, respectively.

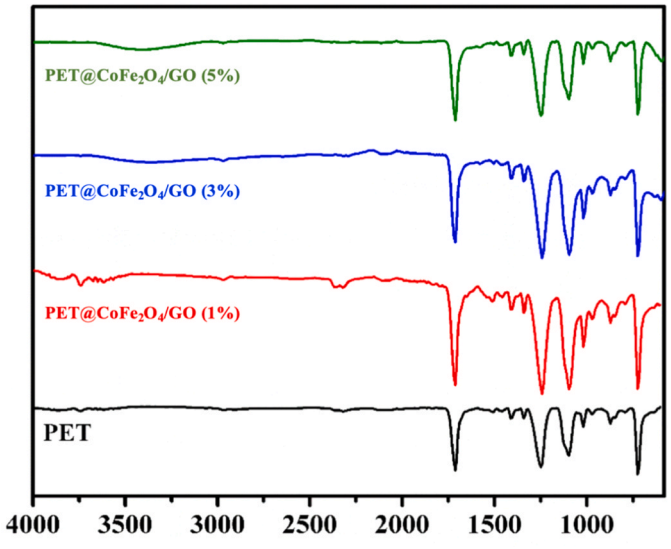

Fig. 2. FTIR spectra of PET, PET@$CoFe_2O_4$/GO (1 %), PET@$CoFe_2O_4$/GO (3 %) and PET@$CoFe_2O_4$/GO (5 %).

Similar FTIR data were reported for pristine PET fabric [32]. Interestingly, other bonds are also observed at 1096 and 1242 cm^{-1}, these last are ascribed to the elongation vibration of the C═O bond of the ester moiety [33]. The elongation vibration of the C═C bond of aromatic ring is characterized by the band located at 1420 cm^{-1}. Finally, the located band at 1712 cm^{-1} represents the C═O bond vibration of the aromatic ester group [34].

After $CoFe_2O_4$/GO coating, several changes appeared in the FTIR spectra of coated samples, including the peak at 3380 cm^{-1}, ascribed to the hydroxyl groups (O-H). This band increases in terms of intensity with increasing the amount of $CoFe_2O_4$/GO which confirms its successful deposition on the polyester fabric, suggesting a strong adhesion between PET fabric and $CoFe_2O_4$/GO coating, originated either from the non-covalent interaction generally occurring between aromatic moieties of polymers and graphitic structures either from (1) π–π stacking [35,36] or (2) generated from the Van der Waals force between polyester and graphite which was proved to perform a compelling role in adhesion [37]. The XRD patterns of pristine PET and coated PET fabrics are illustrated in Fig. 3. The recorded XRD patterns showed no change in the diffraction peak of PET after loading with $CoFe_2O_4$/GO, indicating that the $CoFe_2O_4$/GO coating did not affect the PET crystallinity. However, in line with recent studies, the XRD of coated PET has shown the emergence of new, distinct diffraction peaks at 35.6°, 43.3°, 57.1°, and 62.9°. These peaks are attributed to (311), (400), (333), and (440), respectively, and reveal reflections from the cubic spinel structure of cobalt ferrite [38,39]. It should be noted that the diffraction peak intensity increases with increasing the coating loading from 1 % to 5 %. According to the JCPDS card No. 22–1086, the new peaks are matching to the crystal planes of the $CoFe_2O_4$ cubic spinel-type structure.

3.2. Morphological analysis

The colour changes of all PET samples were observed and measured by colour coordinates. Table 1 presents data COLOR of pristine and coated PET samples. It is well observed that the colour coordinates

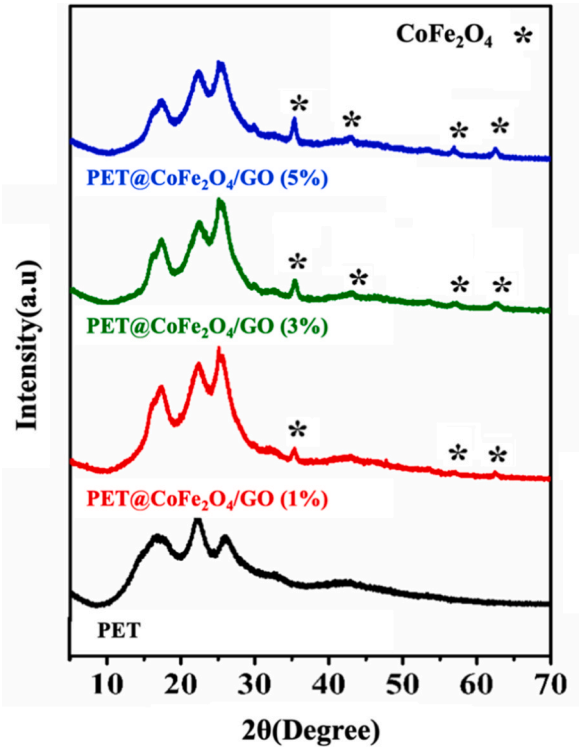

Fig. 3. XRD patterns of PET, $CoFe_2O_4$/GO (1 %), $CoFe_2O_4$/GO (3 %) and $CoFe_2O_4$/GO (5 %).

Table 1
Colour coordinates (data COLOR) of the pristine PET and the prepared PET@G-ODA fabrics.

PET Samples	Colour coordinates		
	L*	a*	b*
PET	87.31	1.02	0.77
PET@$CoFe_2O_4$/GO (1 %)	58.98	1.78	3.67
PET@$CoFe_2O_4$/GO (3 %)	37	2.26	4.67
PET@$CoFe_2O_4$/GO (5 %)	27.88	3.44	6.40

values of PET changed after $CoFe_2O_4$/GO coating, demonstrating the colour differences between the uncoated sample and the coated ones. The pristine PET sample showed a value of lightness L*= 87.31, which is almost the same value found in the literature [40]. This value is the highest compared to PET@ $CoFe_2O_4$/GO (1 %), PET@$CoFe_2O_4$/GO (3 %) and PET@$CoFe_2O_4$/GO (5 %), which showed values of L* equal to 58.98, 37 and 27.88, respectively, describing that the coating with $CoFe_2O_4$/GO lead to a decreased lightness value for the coated PET fabrics. The values of a* (redness-greenness) and b* (yellowness-blueness) changed as well after coating, from (a*= 1.02, b*=0.77) for the uncoated fabric to (a*= 1.78, b*=3.67), (a*= 2.26, b*=4.67) and (a*= 3.44, b*=6.40) for PET@$CoFe_2O_4$/GO (1 %), PET@$CoFe_2O_4$/GO (3 %) and PET@$CoFe_2O_4$/GO (5 %), respectively, which is in good accordance with our previous related works [41]. Furthermore, by comparing the colour coordinates values as well as the digital images in Fig. 1. It can be observed that the colour of the PET pristine increases with increasing the loading of $CoFe_2O_4$/GO from 1 % to 5 %, which affirms the successful deposition of $CoFe_2O_4$/GO on the PET fabric's surface.

To study the surface morphology of pristine and coated fabrics as well as the $CoFe_2O_4$/GO coating uniformity on the surface of coated fibres, SEM observation was investigated. Fig. 4. displays the SEM images of uncoated PET samples, PET@$CoFe_2O_4$/GO (1 %), PET@$CoFe_2O_4$/GO (3 %) and PET@$CoFe_2O_4$/GO (5 %). The uncoated PET consisted of entangled microfibers with relatively clean and smooth surfaces as shown in Fig. 4**(a)**. However, after coating with $CoFe_2O_4$/GO hybrid, the PET surface was fully wrapped with $CoFe_2O_4$/GO and became thicker and most of the wires were covered with increasing the coating amount. $CoFe_2O_4$/GO coating appears to modify the surface morphology of the fibres and renders the textiles' surface rougher due to the presence of GO nanosheets and $CoFe_2O_4$ nanoparticles. This trend was also observed in similar GO-coated fabrics [42,43]. These findings show that $CoFe_2O_4$/GO adheres to the PET surface successfully. Using the elemental mapping method, the element distribution of C, O, Fe, and Co elements in coated PET with $CoFe_2O_4$/GO hybrid was examined. As illustrated in Fig. 5, the distribution of C, O, Fe and Co elements for the PET fabric coated with $CoFe_2O_4$/GO hybrid material is uniform on the fibre's surface and fills the fibre's gaps.

3.3. Thermogravimetric analysis

The thermal stability of all PET samples was studied through thermogravimetric analysis (TGA). Fig. 6 displays the TGA and DTG thermograms of all prepared samples: PET, PET@$CoFe_2O_4$/GO (1 %), PET@$CoFe_2O_4$/GO (3 %) and PET@$CoFe_2O_4$/GO (5 %) and Table 2 gathers the temperature designating 10 % ($T_{10\,\%}$) and 50 % ($T_{50\,\%}$) weight loss. From the obtained results, no change was observed in the TGA analysis curves in the range of 0–300 °C before and after $CoFe_2O_4$/GO coating, suggesting that the coating doesn't alter or affect the quality of the fibre, nor the PET native properties in the range of the temperature of the desired application. Similar results were reported in our previous PET-coated GO studies [8], in which the graphene-based coating approach successfully improved the overall thermal stability of the PET fabrics by establishing strong interactions with PET fibre. Based on the TGA and DTG curves, it is seen that the thermograms present identical shapes as

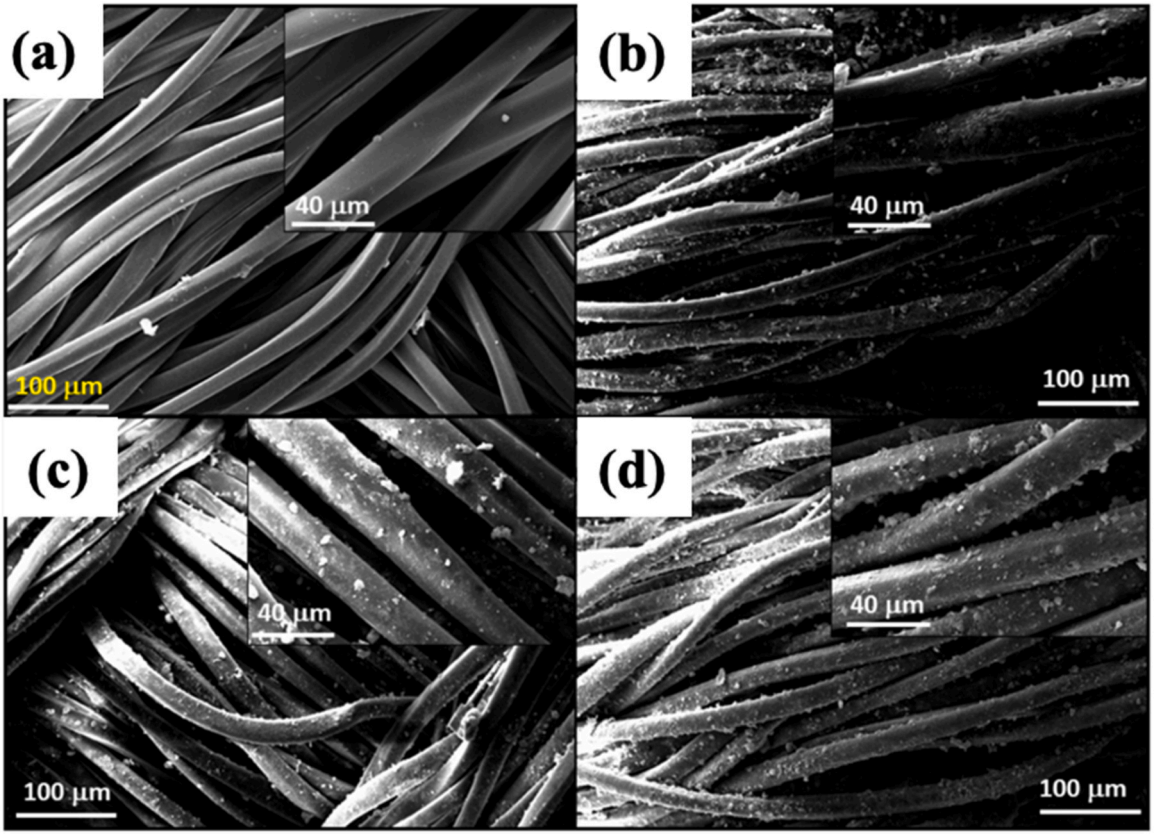

Fig. 4. SEM images of (a) PET, (b) $CoFe_2O_4$/GO (1 %), (c) $CoFe_2O_4$/GO (3 %) and (d) $CoFe_2O_4$/GO (5 %).

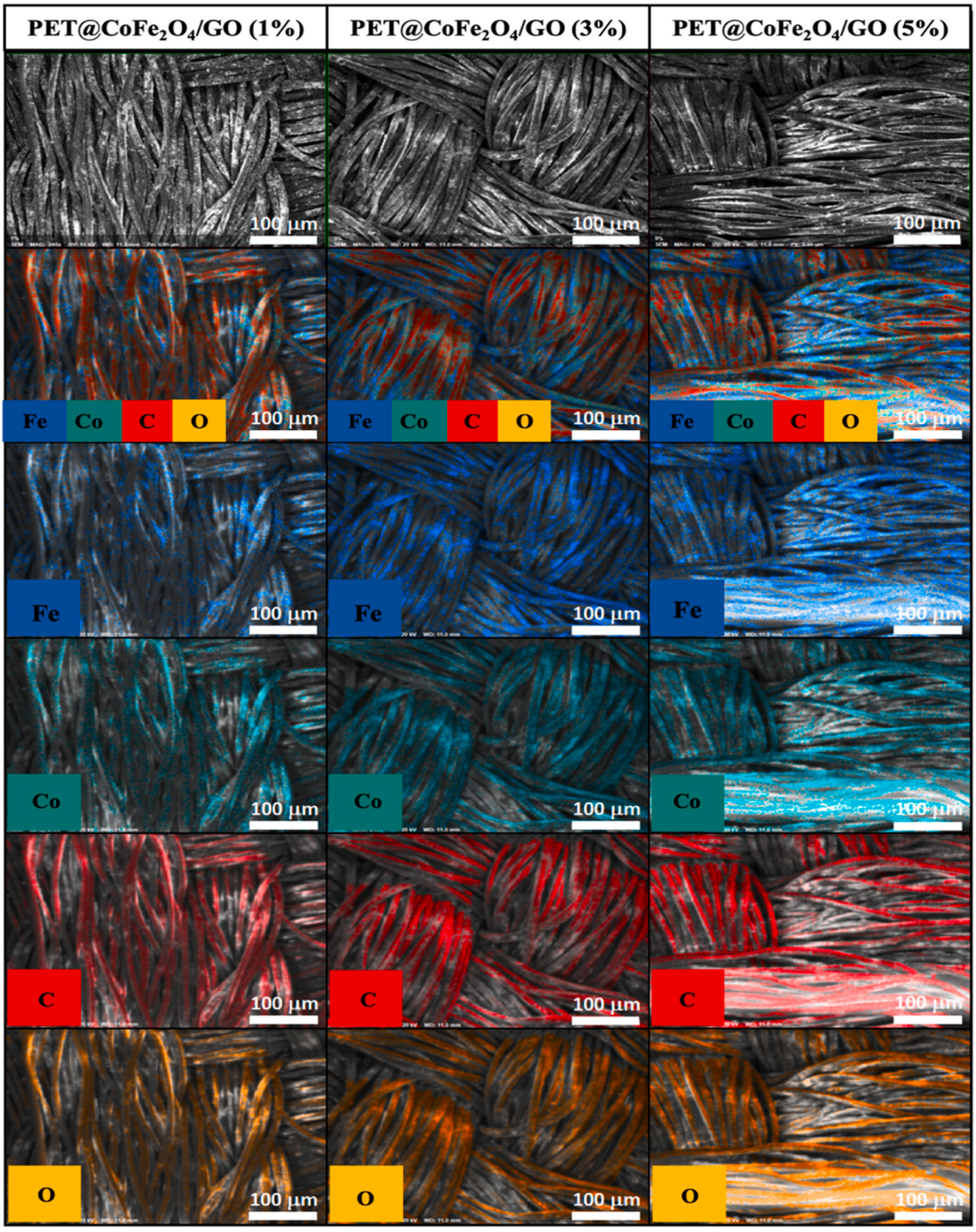

Fig. 5. X-ray mapping images of coated PET@$CoFe_2O_4$/GO textiles.

well as the appearance of two peaks at the range from 350 to 600 °C, indicating that the fabrics' degradation takes place in two stages. The first one recorded from 350 to 480 °C, which is assigned to the depolymerisation and reaction of simultaneous β CH-transfer [44]. The second one, occurring between 480 and 550 °C belongs to the char oxidation that is formed during the first weight loss phase. Moreover, to further investigate the thermal stability and the degradation behaviour of pristine and coated textile fabrics at higher temperatures, the temperatures $T_{10\,\%}$ and $T_{50\,\%}$, corresponding to 10 % and 50 % weight losses of uncoated and coated samples were compared. By comparing pristine PET and coated ones, it is noticed that these last decompose at a quite higher temperature. Indeed, the temperature corresponding to 10 % weight loss increased by 33.29 °C for PET@ $CoFe_2O_4$/GO (1 %), 34, 58 °C for both PET@ $CoFe_2O_4$/GO (3 %) and PET@ $CoFe_2O_4$/GO (5 %) coated samples. From the obtained results, it can be concluded that the incorporation of $CoFe_2O_4$/GO hybrid allows an improvement of PET thermal stability after coating, which is manifested by an increase of degradation temperatures, and maintains this property independently of coating amount, confirming the good adhesion and compatibility between $CoFe_2O_4$/GO and the macromolecular chains of PET. Such results

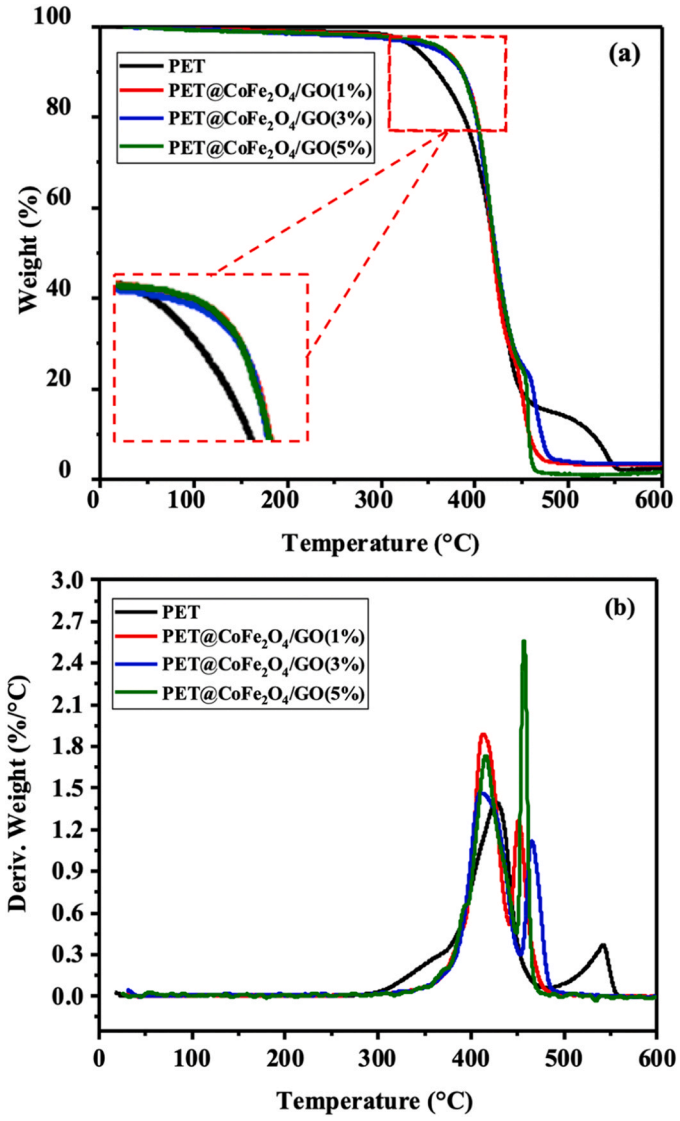

Fig. 6. (a) TGA and (b) DTG thermograms of PET, PET@ $CoFe_2O_4$/GO (1 %), PET@ $CoFe_2O_4$/GO (3 %) and PET@ $CoFe_2O_4$/GO (5 %).

Table 2
Thermal analysis data of PET, PET@$CoFe_2O_4$/GO (1 %), PET@$CoFe_2O_4$/GO (3 %) and PET@$CoFe_2O_4$/GO (5 %).

Samples	PET	PET@$CoFe_2O_4$/GO (1 %)	PET@$CoFe_2O_4$/GO (3 %)	PET@$CoFe_2O_4$/GO (5 %)
$T_{10\,\%}$ (°C)	352.66	385.95	387.24	487.24
$T_{50\,\%}$ (°C)	421.34	421.34	421.34	421.34

might be due to graphene's intrinsic properties, leading to the enhancement of the thermal properties of textile fabrics [45].

3.4. Performance of cobalt-ferrites/graphene oxide-coated fabric

3.4.1. Tensile test

The tensile tests were realized to evaluate and investigate the tensile properties of the treated fabrics, compared to pristine samples. Tensile strength, elongation at the break and Young's modulus, of coated and uncoated fabrics were evaluated and presented in Fig. 7 and Table 3. According to the results, all coated PET samples showed a small

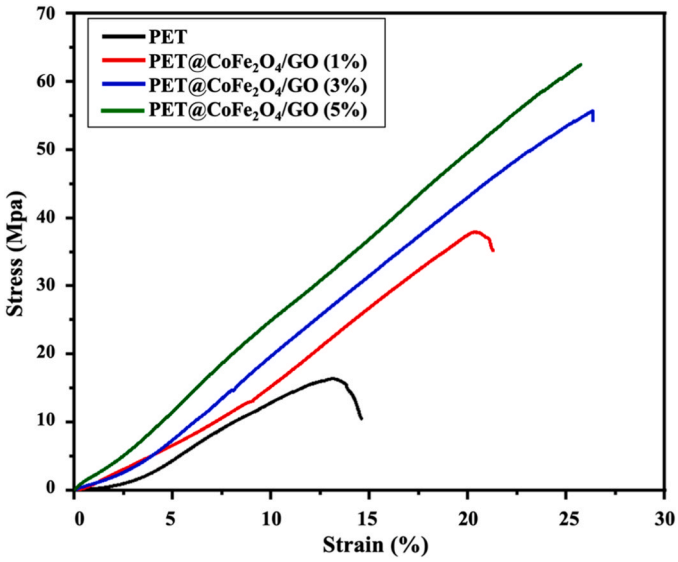

Fig. 7. Stress-strain curves of PET, PET@$CoFe_2O_4$/GO (1 %), PET@$CoFe_2O_4$/GO (3 %) and PET@$CoFe_2O_4$/GO (5 %).

Table 3
Tensile test parameters of pristine and coated PET fabrics.

Samples	Elongation at break (%)	Young's modulus (MPa)	Stress at the fracture point (MPa)
PET	14.59 ± 1.96	154.6 ± 0.01	16.38 ± 0.88
PET@$CoFe_2O_4$/GO (1 %)	21.24 ± 2.28	214.7 ± 0.017	38.03 ± 1.45
PET@$CoFe_2O_4$/GO (3 %)	26.81 ± 1.41	230.6 ± 0.08	56.05 ± 1.12
PET@$CoFe_2O_4$/GO (5 %)	26.37 ± 1.21	249.1 ± 0.23	62.29 ± 1.6771

improvement in tensile strength and Young's modulus when compared to virgin PET. The developed PET@$CoFe_2O_4$/GO fabric's tensile strength has improved with increasing the $CoFe_2O_4$/GO loading from 1 % to 5 %, which increased the GO amount on the surface of the PET substrate, leading to improved mechanical performance, as it has also been reported in previously [46]. Indeed, after coating, the tensile strength (Rm) increased from 16.38 ± 0.88 MPa for the uncoated PET sample, to 38.03 ± 1.45 Mpa, 56.05 ± 1.12 Mpa and 62.29 ± 1.67 Mpa, for PET@$CoFe_2O_4$/GO (1 %), PET@$CoFe_2O_4$/GO (3 %) and PET@$CoFe_2O_4$/GO (5 %), respectively.

Similarly, an increase in the elongation at break was observed for the treated fabrics compared to pristine ones, with values of 14.59 % for neat PET, 21.24 % for PET@$CoFe_2O_4$/GO (1 %), 26.81 % for PET@$CoFe_2O_4$/GO (3 %) and 26.37 % PET@$CoFe_2O_4$/GO (5 %). The prepared fabrics in our study presented better results compared to other graphene-coated fabrics [47], suggesting the efficiency of the adopted coating technique as well as the coating's good uniformity in the surface of the PET fibres, which was observed by SEM images. The Young's modulus value, which was calculated from the elastic domain [48], also increased significantly from 154.6 ± 0.01Mpa for pristine PET to 249.1 ± 0.23Mpa for PET@$CoFe_2O_4$/GO (5 %) coated fabric, showing that the coating improved significantly the over-all mechanical properties of the PET sample. This suggests that $CoFe_2O_4$/GO coating generates a layer at the surface of the fabric, that in turn ameliorates its mechanical properties, which is expected to be, knowing the excellent mechanical characteristics of graphene, transferred to the coated fabrics [49].

3.4.2. Catalytic activity

To investigate the catalytic performance of our elaborated textile

fabrics, RhB degradation in the presence of PMS was selected as a model representative catalytic reaction based on our recent study [26]. The RhB solution degradation kinetics was investigated by tracking the decrease in the RhB peak at 554 nm via UV–vis spectra as a function of time (Fig. 8**(a)**). Additionally, the curve of standard calibration (R^2=0.976) verified the linear relationship between the absorbance of the remaining RhB and its concentration, and the acquired absorbance was subsequently translated to RhB concentration. From our previous work [26], it is confirmed that no RhB degradation was seen neither in the absence of PMS, nor $CoFe_2O_4$/GO catalyst. Furthermore, in the absence of the catalyst, the RhB degradation reaction by PMS alone was not possible. When the complete system—PMS and catalyst—is present, the degradation process is most efficient. According to Fig. 8**(b)**, an obvious decrease in the initial concentration was observed as well as a clear colour change in the RhB solution (Fig. 9). The RhB solution's initial concentration was 15 ppm. After 2 min reaction, using PET@-$CoFe_2O_4$/GO, the concentration decreased significantly to 8.12 ± 0.03 ppm and continued decreasing to reach 0.52 ± 0.04 ppm after only 10 min reaction. Suggesting the effectiveness of PET@$CoFe_2O_4$/GO as a catalytic for RhB degradation, which is in agreement with what was found in a previous study [26].

To investigate and clarify the RhB degradation, TOC, which is an important parameter that describes the mineralization degree of organic species, was utilized to study the process of RhB degradation by the PMS-PET@$CoFe_2O_4$/GO system. Fig. 10. shows the TOC removal of RhB from the aqueous solution using PMS, in the presence of PET@$CoFe_2O_4$/GO (5 %). The TOC removal reached 59.17 % in only 4 min and significantly increased with time increasing, to reach 89.82 % after only 12 min reaction. These results confirm that the coated PET fabric could mineralize RhB to residual organic molecules which is in total accordance with our recent study [26], in which the TOC removal efficiency was about 89.34 % in the presence of PMS/$CoFe_2O_4$/GO system. The observed high catalytic activity of coated PET@$CoFe_2O_4$/GO (5 %) fabric is mainly related to both $CoFe_2O_4$ nanoparticles and GO contribution to the improvement of the catalytic activity of $CoFe_2O_4$ catalyst by providing more active sites for catalytic RhB degradation [50]. Moreover, the incorporation of $CoFe_2O_4$/GO onto textiles fabrics guarantees the easy separation process, of the as-prepared catalyst from the final solution without the necessity of applying an external magnetic field [51], which is required especially in scalable applications.

To further study the re-usability of our elaborated fabrics, the catalytic degradation experiment was performed and TOC removal was calculated after several reusability cycles of 12 min, using the same PET@$CoFe_2O_4$/GO under the same conditions: $[RhB]_0$ = 0.03 mmol/L, amount of deposited $CoFe_2O_4$/GO on textile sample =10 mg, [PMS]= 0.10 mg/L, temperature =25 °C. After each 12 min, the PET@$CoFe_2O_4$/GO textile was removed from the treated solution and cleaned with water, then reused again for other RhB removal cycle, as shown in Fig. 11. The degradation rate of RhB was still over 60 % even after 7 cycles, suggesting that no loss of metal-catalyzed occurred, neither leaching of cobalt ion from the $CoFe_2O_4$/GO structure, which is limiting the re-usability of the catalyst as observed for some co-based catalyst previously reported in literature [52]. The obtained results suggest the important role of textile support, preventing the loss of the catalyst and enhancing reusability, thus leading to cost-effectiveness. However, the present research on the development of PET supported catalyst for RhB degradation is still at an early stage, more investigations about the effect of influencing parameters such as solution's initial pH, PMS concentration, reaction time and PET@$CoFe_2O_4$/GO catalyst amount needs to be further studied. Up till now, the successful immobilization of $CoFe_2O_4$/GO onto PET fabrics showed, not only high catalytic activity for the degradation of RhB but also a good re-usability of the developed PET@$CoFe_2O_4$/GO in several successive degradation cycles. These results are very promising and could allow the development of a new generation of powerful multifunctional fabrics, known as textile catalysts.

3.4.3. Antibacterial activity

The antibacterial properties of coated PET fabrics were determined by investigating the formed inhibition zone by a direct method with Gram-positive (*S.aureus*) and Gram-negative (*E.coli*) on agar medium. The obtained results of this study are presented in Fig. 12., the reference sample was the pristine PET, which showed no inhibition zone, with a clear bacterial growth. The bacteria surrounding and beneath the modified PET@$CoFe_2O_4$/GO samples were eliminated, as seen by the distinct circular regions devoid of bacterial growth. In both Gram-positive and Gram-negative organisms, distinct inhibition zones were observed, and for PET@$CoFe_2O_4$/GO (5 %) the inhibition diameter reached 13 mm. The observed findings are comparable to a recent work on PET fabric functionalized with silver nanoparticles and graphene, in which the authors reported inhibition zones between 1.75 and 12 mm, against *S.aureus* [53]. In another similar work, Ouadil et al. [41] reported the fabrication of a coated with graphene/silver nanoparticles PET fabric. The authors reported lower antibacterial efficiency, compared to the obtained results in our work, against both *S.aureus* and *E.coli* bacteria with an inhibition diameter of 10 mm. These findings may be explained by the exceptional antibacterial activity of $CoFe_2O_4$ nanoparticles, which has been demonstrated in prior published studies

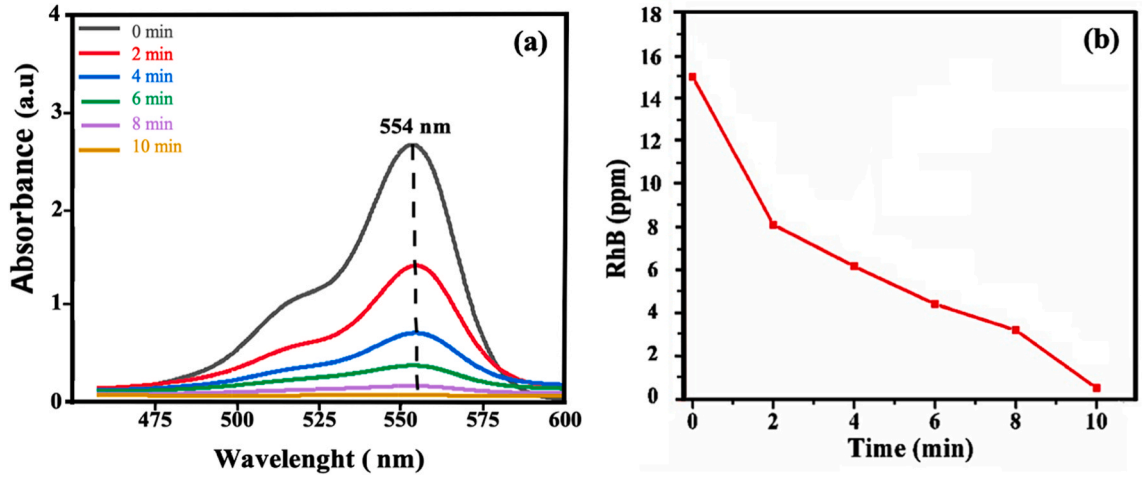

Fig. 8. (a) UV–vis spectra (b) change in concentration and absorbance as a function of time. Reaction Conditions: [PMS]=0.10 mg/L, amount of deposited $CoFe_2O_4$/GO on textile sample =10 mg, $[RhB]_0$ = 0.03 mmol/L,temperature =25 °C.

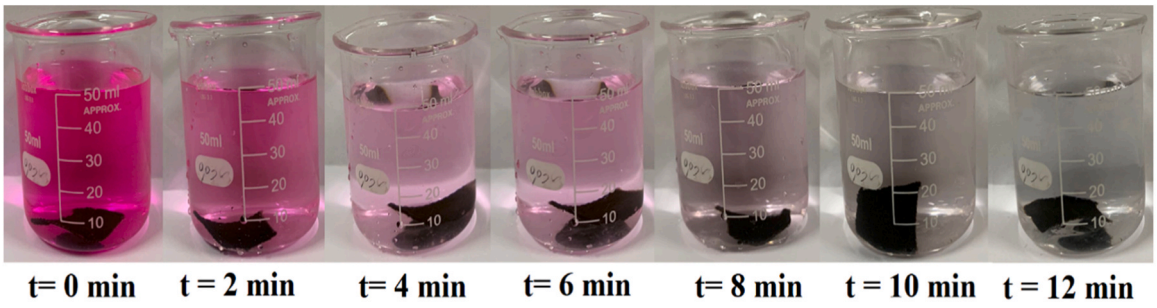

Fig. 9. Images of RhB solution before, during and after using PET@$CoFe_2O_4$/GO (5 %) as a catalyst.

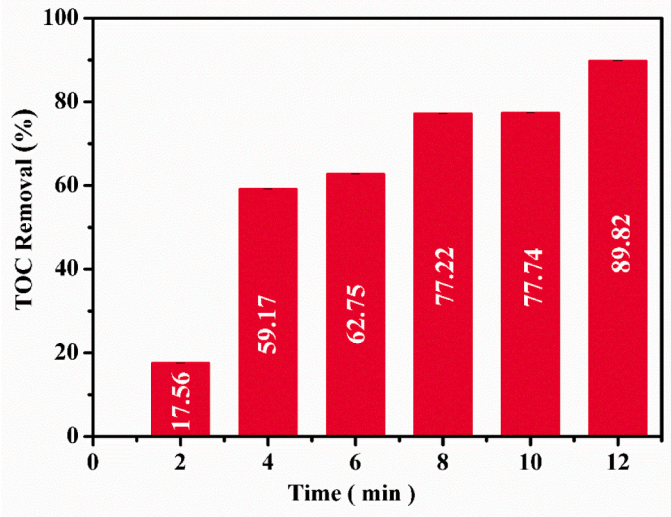

Fig. 10. TOC removal efficiency of RhB using PET@$CoFe_2O_4$/GO. Reaction conditions; [PMS]=0.10 mg/L, amount of deposited $CoFe_2O_4$/GO on textile sample =10 mg, $[RhB]_0$ = 0.03 mmol/L,temperature =25 °C.

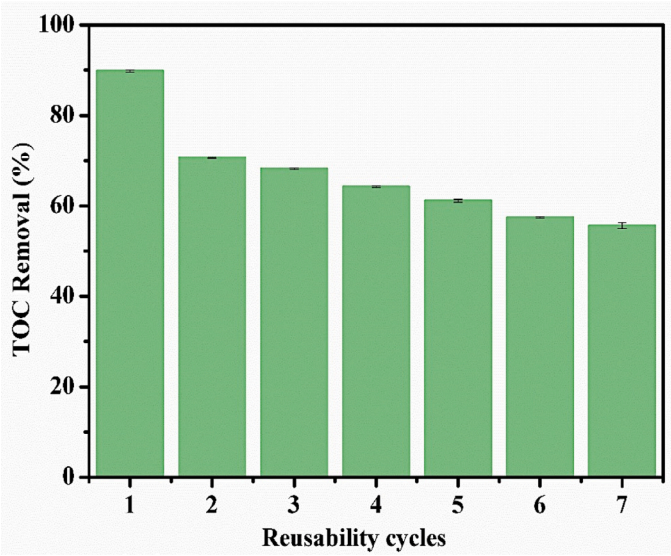

Fig. 11. Reuse performance of PET@$CoFe_2O_4$/GO catalyst in RhB degradation reaction.

against a variety of microbes [23]. According to the current study, GO also gives textiles a high specific area and hydrophobic property, which improves barrier qualities and lowers the growth and adherence of germs on PET samples [54,55].

3.4.4. *Coating durability*

Washing is considered one of the crucial obstacles that limit the growth of coated fabrics in industrial applications. It is well known that washing could easily deteriorate the coating structure and accelerate its detachment from the textile substrate [56]. Washing tests were also performed to investigate the effect of washing on our elaborated PET@$CoFe_2O_4$/GO (5 %) compared to pristine PET, against several cycles of washing. The samples were subjected to washing for 1 h hour each, under vigorous stirring. The PET@$CoFe_2O_4$/GO (5 %) sample's weight was first measured and put in 100 mL solutions of hot water (100 °C) and detergent as washing media, for 15 cycles. After each cycle, the sample was rinsed, dried and measured to obtain its final weight after washing to calculate the weight loss. From Fig. 13, it can be observed that the textile's initial weight remained approximately the same, with only a slight decrease, after 15 washing cycles.

For the pristine fabric, after 15 cycles, the weight loss, corresponding to 1.32 % for hot water and 2.27 % for detergent, may be due to dirt and impurities, remaining after the pre-treatment of the PET fabric. These impurities are removed more and more by increasing the washing cycles. After the first cycle, the weight loss using hot water as a washing medium is 0.37 % and 0.68 % using detergent. After 15 cycles, the weight loss increased to 1.32 % and 1.58 %, respectively for hot water and detergent, which is in agreement with the suggestion and explains the weight loss corresponding to the pristine fabric. The accumulated weight loss might also be attributed to the probably damaged structure under the as-followed washing conditions (vigorous stirring, 1 h/ cycle). Such findings were obtained also in the previous works [57].

For the coated PET@$CoFe_2O_4$/GO (5 %), the observed accumulated weight loss of 2.49 %, after 15 cycles using hot water, was mainly due to the coating removal, which was caused by the vigorous stirring for 1 hour, leading to the coating removal. Compared to coated PET@$CoFe_2O_4$/GO (5 %), pristine PET fabric exhibited superior weight loss (2.27 % For PET and 1.58 % for PET@$CoFe_2O_4$/GO (5 %)) using detergent as washing media, which can be probably explained by, the removal of the remained dirt and impurities in the fabrics and also the possible structural damage caused by the washing conditions. Unlike the PET@$CoFe_2O_4$/GO (5 %), the presence of the covering layer of $CoFe_2O_4$/GO, may play the protection role, protecting the internal fibres against the proliferation of the detergent and thus, removing only the coating layer. From Fig. 13 it is observed that the coated textile's initial weight remained approximately the same, after 15 accumulated cycles of washing, with only a slight decrease, 2.49 % for hot water and 1.58 % for detergent, these findings indicated the durability of $CoFe_2O_4$/GO coating on PET.

4. Conclusion

The functionalization of PET fabrics was carried out using an easy dip-coating method in $CoFe_2O_4$/GO solution. The effective coating of the fabrics, the improvement of mechanical characteristics, the

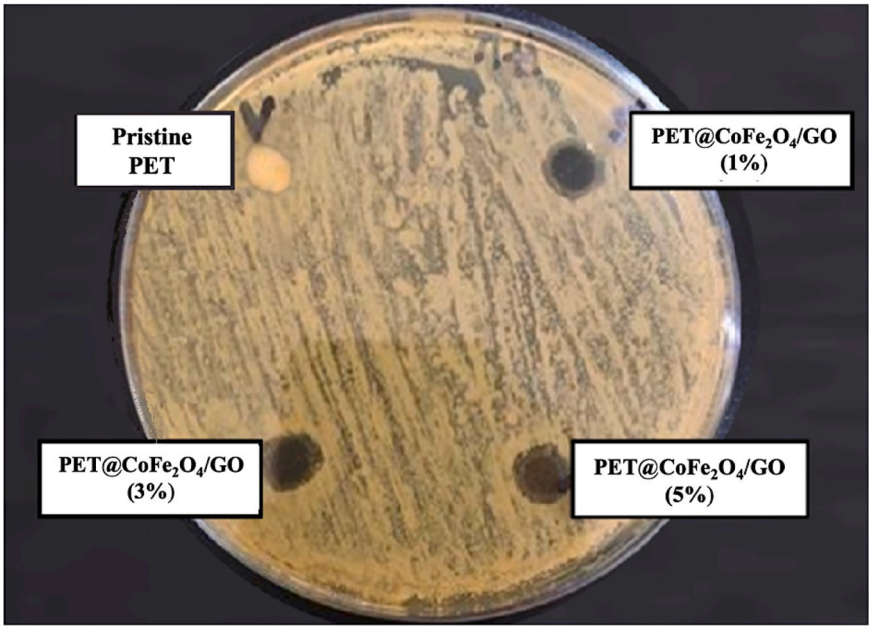

Fig. 12. Antibacterial activity of pristine and coated PET.

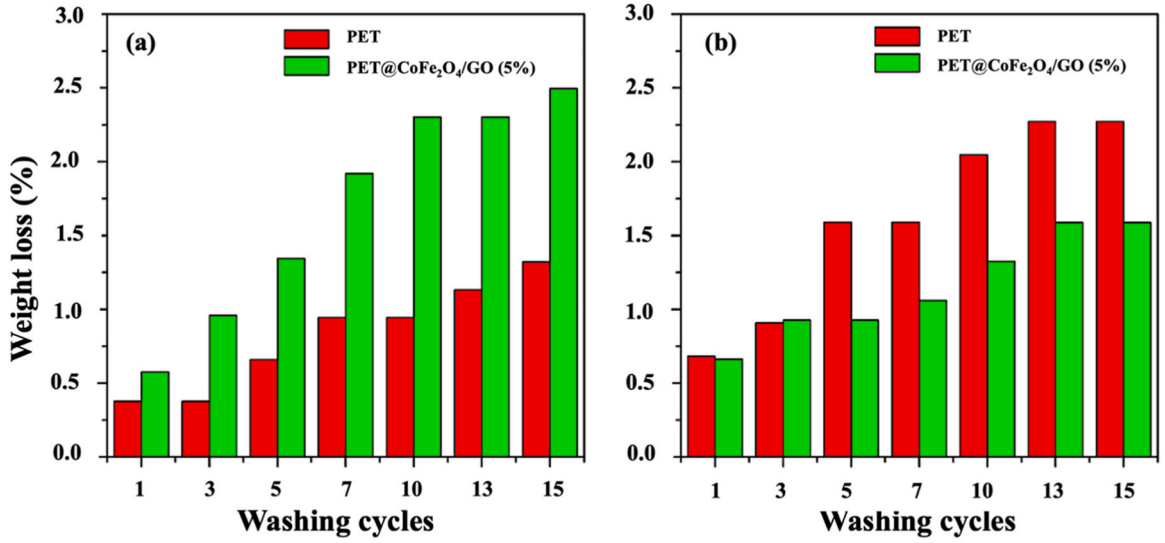

Fig. 13. PET@$CoFe_2O_4$/GO (5 %) washing test using (a) hot water and (b) detergent.

improvement of thermal stability, and the immaculate PET have all been confirmed by physio-chemical characterisation techniques. The created textiles showed exceptional catalytic activity for PMS activation in the RhB degradation reaction, removing 89.82 % of the TOC in 12 minutes of reaction time. What's more, the developed coated fabrics demonstrated good reusability. Furthermore, due to the well-known antibacterial activity of $CoFe_2O_4$ nanoparticles, the coated PET@$CoFe_2O_4$/GO, loaded from 1 % to 5 % wt, demonstrated exceptional antibacterial effectiveness against Staphylococcus aureus and Escherichia coli germs, with an inhibitory diameter of 13 mm. The PET@$CoFe_2O_4$/GO coated textiles are thus combining catalytic and anti-bacterial properties, with a potential application in the removal of hazardous organic compounds and growth inhinition of microorganisms in wastewater. The research in textiles-supported catalysts is in the early stages, more research must be conducted mainly to understand the fundamentals of the catalyst coating process, thus allowing the design of long-lasting catalytic supports with high activity and suitable for scientific and industrial applications.

CRediT authorship contribution statement

Ghizlane Achagri: Writing – original draft, Software, Methodology, Formal analysis, Data curation, Conceptualization. **Othmane Dardari:** Writing – original draft, Software, Methodology, Formal analysis. **Othmane Amadine:** Writing – original draft, Methodology, Formal analysis, Conceptualization. **Abudukeremu Kadier:** Writing – review & editing- Supervision, Resources. **Younes Essamlali:** Writing – original draft, Investigation, Conceptualization. **Ghita Radi Benjelloun:** Formal analysis, Biological tests. **Mohamed Zahouily:** Writing – review & editing, Validation, Project administration, Data curation, Funding acquisition, Conceptualization. **Farooq Sher:** Writing – review & editing, Funding acquisition, Project administration.

Declaration of Competing Interest

The authors declare that they have no known competing financial interests or personal relationships that could have appeared to influence the work reported in this paper.

Data Availability

Data will be made available on request.

Acknowledgements

The authors are grateful for the financial support from the administrative, technical and financial assistance of University Hassan II of Casablanca and the Moroccan Foundation for Advanced Science, Innovation and Research (MAScIR). The supports from International Society of Engineering Science and Technology (ISEST) UK, towards this research are hereby acknowledged. The authors are also grateful for the financial support from the Tianchi Doctor Program of Xinjiang Uygur Autonomous Region, and the National Foreign Young Talents Program-Department of Foreign Expert Services of the Ministry of Science and Technology, China (QN2023046003L).

References

[1] H.A. Al-Gaoudi, M.A. Marouf, N. Badry, M. Rehan, Design innovative strategies for coating archaeological linen textiles surface to achieve protective multifunctional properties, J. Cult. Herit. 59 (2023) 274–286, https://doi.org/10.1016/j.culher.2023.01.002.

[2] D. Xu, Z. Ouyang, Y. Dong, H.-Y. Yu, S. Zheng, S. Li, K.C. Tam, Robust, breathable and flexible smart textiles as multifunctional sensor and heater for personal health management, Adv. Fiber Mater. 5 (2023) 282–295, https://doi.org/10.1007/s42765-022-00221-z.

[3] Z. Wang, Y. Huang, J. Sun, Y. Huang, H. Hu, R. Jiang, W. Gai, G. Li, C. Zhi, Polyurethane/cotton/carbon nanotubes core-spun yarn as high reliability stretchable strain sensor for human motion detection, ACS Appl. Mater. Interfaces 8 (2016) 24837–24843, https://doi.org/10.1021/acsami.6b08207.

[4] G. Zheng, Y. Cui, Z. Jiang, M. Zhou, P. Wang, Y. Yu, Q. Wang, Multifunctional composite coatings with hydrophobic, UV-resistant, anti-oxidative, and photothermal performance for healthcare, Colloids Surf. A: Physicochem Eng. Asp. 667 (2023) 131367, https://doi.org/10.1016/j.colsurfa.2023.131367.

[5] M. Salat, P. Petkova, J. Hoyo, I. Perelshtein, A. Gedanken, T. Tzanov, Durable antimicrobial cotton textiles coated sonochemically with ZnO nanoparticles embedded in an in-situ enzymatically generated bioadhesive, Carbohydr. Polym. 189 (2018) 198–203, https://doi.org/10.1016/j.carbpol.2018.02.033.

[6] H. Shayesteh, M.S. Khosrowshahi, H. Mashhadimoslem, F. Maleki, Y. Rabbani, H.B. M. Emrooz, Durable superhydrophobic/superoleophilic melamine foam based on biomass-derived porous carbon and multi-walled carbon nanotube for oil/water separation, Sci. Rep. 13 (2023) 4515, https://doi.org/10.1038/s41598-023-31770-x.

[7] Y.-N. Gao, Y. Wang, T.-N. Yue, Y.-X. Weng, M. Wang, Multifunctional cotton nonwoven fabrics coated with silver nanoparticles and polymers for antibacterial, superhydrophobic and high performance microwave shielding, J. Colloid Inter Sci. 582 (2021) 112–123, https://doi.org/10.1016/j.jcis.2020.08.037.

[8] G. Achagri, Y. Essamlali, O. Amadine, M. Majdoub, A. Chakir, M. Zahouily, Surface modification of highly hydrophobic polyester fabric coated with octadecylamine-functionalized graphene nanosheets, RSC Adv. 10 (2020) 24941–24950, https://doi.org/10.1039/D0RA02655G.

[9] Q. Bao, Z. Yang, Z. Lu, X. He, Effects of graphene thickness and length distribution on the mechanical properties of graphene networks: a coarse-grained molecular dynamics simulation, Appl. Surf. Sci. 570 (2021) 151023, https://doi.org/10.1016/j.apsusc.2021.151023.

[10] H. Ruan, A. Aulova, V. Ghai, S. Pandit, M. Lovmar, I. Mijakovic, R. Kádár, Polysaccharide-based antibacterial coating technologies, Acta Biomater. (2023) S1742706123004087, https://doi.org/10.1016/j.actbio.2023.07.023.

[11] H. Jung, G. Shin, H. Kwak, L.T. Hao, J. Jegal, H.J. Kim, H. Jeon, J. Park, D.X. Oh, Review of polymer technologies for improving the recycling and upcycling efficiency of plastic waste, Chemosphere 320 (2023) 138089, https://doi.org/10.1016/j.chemosphere.2023.138089.

[12] S. Some, R. Mondal, D. Mitra, D. Jain, D. Verma, S. Das, Microbial pollution of water with special reference to coliform bacteria and their nexus with environment, Energy Nexus 1 (2021) 100008, https://doi.org/10.1016/j.nexus.2021.100008.

[13] T. Münzel, O. Hahad, A. Daiber, P.J. Landrigan, Soil and water pollution and human health: what should cardiologists worry about? Cardiovasc Res. 119 (2023) 440–449, https://doi.org/10.1093/cvr/cvac082.

[14] M.A. Barros, C.L. Seabra, M.J. Sampaio, C. Nunes, C.G. Silva, S. Reis, J.L. Faria, Eradication of gram-negative bacteria by reusable carbon nitride-coated cotton under visible light, Appl. Surf. Sci. (2023) 157311, https://doi.org/10.1016/j.apsusc.2023.157311.

[15] M. Peydayesh, M.K. Suter, S. Bolisetty, S. Boulos, S. Handschin, L. Nyström, R. Mezzenga, Amyloid fibrils aerogel for sustainable removal of organic contaminants from water, Adv. Mater. 32 (2020) 1907932, https://doi.org/10.1002/adma.201907932.

[16] A.A. Al-Gheethi, Q.M. Azhar, P.S. Kumar, A.A. Yusuf, A.K. Al-Buriahi, R. M. Mohamed, M.M. Al-shaibani, Sustainable approaches for removing Rhodamine B dye using agricultural waste adsorbents: a review, Chemosphere (2022) 132080, https://doi.org/10.1016/j.chemosphere.2021.132028.

[17] S. Ammar, A. Helfen, N. Jouini, F. Fiévet, I. Rosenman, F. Villain, P. Molinié, M. Danot, Magnetic properties of ultrafine cobalt ferrite particles synthesized by hydrolysis in a polyol medium, J. Mater. Chem. 11 (2001) 186–192, https://doi.org/10.1039/b003193n.

[18] A. El Mouden, N. El Messaoudi, A. El Guerraf, A. Bouich, V. Mehmeti, A. Lacherai, A. Jada, F. Sher, Multifunctional cobalt oxide nanocomposites for efficient removal of heavy metals from aqueous solutions, Chemosphere 317 (2023) 137922, https://doi.org/10.1016/j.chemosphere.2023.137922.

[19] W. Wu, D. Tian, T. Liu, J. Chen, T. Huang, X. Zhou, Y. Zhang, Degradation of organic compounds by peracetic acid activated with Co_3O_4: a novel advanced oxidation process and organic radical contribution, Chem. Eng. J. 394 (2020) 124938, https://doi.org/10.1016/j.cej.2020.124938.

[20] J. Di, R. Jamakanga, Q. Chen, J. Li, X. Gai, Y. Li, R. Yang, Q. Ma, Degradation of rhodamine B by activation of peroxymonosulfate using Co_3O_4-rice husk ash composites, Sci. Total Environ. 784 (2021) 147258, https://doi.org/10.1016/j.scitotenv.2021.147258.

[21] Q.Y. Tamboli, S.M. Patange, Y.K. Mohanta, R. Sharma, K.R. Zakde, Green synthesis of cobalt ferrite nanoparticles: an emerging material for environmental and biomedical applications, J. Nanomater 2023 (2023) 1–15, https://doi.org/10.1155/2023/9770212.

[22] D. Zahn, J. Landers, M. Diegel, S. Salamon, A. Stihl, F.H. Schacher, H. Wende, J. Dellith, S. Dutz, Optimization of magnetic cobalt ferrite nanoparticles for magnetic heating applications in biomedical technology, Nanomaterials 13 (2023) 1673, https://doi.org/10.3390/nano13101673.

[23] D. Gheidari, M. Mehrdad, S. Maleki, S. Hosseini, Synthesis and potent antimicrobial activity of $CoFe_2O_4$ nanoparticles under visible light, Heliyon 6 (2020) e05058, https://doi.org/10.1016/j.heliyon.2020.e05058.

[24] C. Liu, L. Chen, D. Ding, T. Cai, From rice straw to magnetically recoverable nitrogen doped biochar: efficient activation of peroxymonosulfate for the degradation of metolachlor, Appl. Catal. B: Environ. 254 (2019) 312–320, https://doi.org/10.1016/j.apcatb.2019.05.014.

[25] H. Zhang, C. Li, L. Lyu, C. Hu, Surface oxygen vacancy inducing peroxymonosulfate activation through electron donation of pollutants over cobalt-zinc ferrite for water purification, Appl. Catal. B: Environ. 270 (2020) 118874, https://doi.org/10.1016/j.apcatb.2020.118874.

[26] R. Tabit, O. Amadine, Y. Essamlali, K. Danoun, A. Rhihil, M. Zahouily, Magnetic $CoFe_2O_4$ nanoparticles supported on graphene oxide ($CoFe_2O_4$/GO) with high catalytic activity for peroxymonosulfate activation and degradation of rhodamine B, RSC Adv. 10 (2018), https://doi.org/10.1039/c7rao9949e.

[27] W.S. Hummers, R.E. Offeman, Preparation of graphitic oxide, 1339–1339, J. Am. Chem. Soc. 80 (1958), https://doi.org/10.1021/ja01539a017.

[28] L. Gnanasekaran, M. Santhamoorthy, Mu Naushad, Z.A. ALOthman, M. Soto-Moscoso, P.L. Show, K.S. Khoo, Photocatalytic removal of food colorant using NiO/CuO heterojunction nanomaterials, Food Chem. Toxicol. 167 (2022) 113277, https://doi.org/10.1016/j.fct.2022.113277.

[29] G. Achagri, A.E. Idrissi, M. Majdoub, Y. Essamlali, S. Sair, A. Chakir, M. Zahouily, Octadecylamine-functionalized cellulose nanocrystals as durable superhydrophobic surface modifier for polyester coating: Towards oil/water separation, Results Surf. Interfaces (2022) 100061, https://doi.org/10.1016/j.rsurfi.2022.100061.

[30] M.B. Goudjil, H. Dali, S. Zighmi, Z. Mahcene, S.E. Bencheikh, Photocatalytic degradation of methylene blue dye with biosynthesized Hematite α-Fe2O3 nanoparticles under UV-Irradiation, Desalin. Water Treat. 317 (2024) 100079, https://doi.org/10.1016/j.dwt.2024.100079.

[31] T.T. Stubhaug, C.G. Giske, U.S. Justesen, G. Kahlmeter, E. Matuschek, A. Sundsfjord, D. Skaare, Antimicrobial susceptibility testing of Bacteroides species by disk diffusion: the NordicAST Bacteroides study, Anaerobe 81 (2023) 102743, https://doi.org/10.1016/j.anaerobe.2023.102743.

[32] E.S. Allehyani, Y.Q. Almulaiky, S.A. Al-Harbi, R.M. El-Shishtawy, In situ coating of polydopamine-AgNPs on polyester fabrics producing antibacterial and antioxidant properties, Polymers 14 (2022) 3794, https://doi.org/10.3390/polym14183794.

[33] Y.Q. Almulaiky, Polyester fabric modification by chemical treatment to enhancing the β-glucosidase immobilization, Heliyon 8 (2022) e11660, https://doi.org/10.1016/j.heliyon.2022.e11660.

[34] E. Lorusso, W. Ali, M. Hildebrandt, T. Mayer-Gall, J.S. Gutmann, Hydrogel functionalized polyester fabrics by UV-induced photopolymerization, Polymers 11 (2019) 1329, https://doi.org/10.3390/polym11081329.

[35] A. Rahy, P. Bajaj, I.H. Musselman, S.H. Hong, Y.-P. Sun, D.J. Yang, Coating of carbon nanotubes on flexible substrate and its adhesion study, Appl. Surf. Sci. 255 (2009) 7084–7089, https://doi.org/10.1016/j.apsusc.2009.03.048.

[36] B. Shen, W. Zhai, C. Chen, D. Lu, J. Wang, W. Zheng, Melt blending in situ enhances the interaction between polystyrene and graphene through π–π stacking, ACS Appl. Mater. Interfaces 3 (2011) 3103–3109, https://doi.org/10.1021/am200612z.

[37] D.J. Henry, G. Yiapanis, E. Evans, I. Yarovsky, Adhesion between graphite and modified polyester surfaces: a theoretical study, J. Phys. Chem. B 109 (2005) 17224–17231, https://doi.org/10.1021/jp0523524.
[38] R.M. Borade, S.B. Kale, S.U. Tekale, K.M. Jadhav, R.P. Pawar, Cobalt ferrite magnetic nanoparticles as highly efficient catalyst for the mechanochemical synthesis of 2-aryl benzimidazoles, Catal. Commun. 159 (2021) 106349, https://doi.org/10.1016/j.catcom.2021.106349.
[39] V. Mahdikhah, S. Saadatkia, S. Sheibani, A. Ataie, Outstanding photocatalytic activity of $CoFe_2O_4$ /rGO nanocomposite in degradation of organic dyes, Opt. Mater. 108 (2020) 110193, https://doi.org/10.1016/j.optmat.2020.110193.
[40] B. Ouadil, O. Cherkaoui, M. Safi, M. Zahouily, Surface modification of knit polyester fabric for mechanical, electrical and UV protection properties by coating with graphene oxide, graphene and graphene/silver nanocomposites, Appl. Surf. Sci. 414 (2017) 292–302, https://doi.org/10.1016/j.apsusc.2017.04.068.
[41] B. Ouadil, O. Amadine, Y. Essamlali, O. Cherkaoui, M. Zahouily, A new route for the preparation of hydrophobic and antibacterial textiles fabrics using Ag-loaded graphene nanocomposite, Colloids Surf. A: Physicochem Eng. Asp. 579 (2019) 123713, https://doi.org/10.1016/j.colsurfa.2019.123713.
[42] M.A. Al Faruque, A. Kiziltas, D. Mielewski, M. Naebe, A Facile approach of fabricating electrically conductive knitted fabrics using graphene oxide and textile-based waste material, Polymers 13 (2021) 3003, https://doi.org/10.3390/polym13173003.
[43] X. Hu, M. Tian, L. Qu, S. Zhu, G. Han, Multifunctional cotton fabrics with graphene/polyurethane coatings with far-infrared emission, electrical conductivity, and ultraviolet-blocking properties, Carbon 95 (2015) 625–633, https://doi.org/10.1016/j.carbon.2015.08.099.
[44] B.A. Alshammari, F.S. Al-Mubaddel, M.R. Karim, M. Hossain, A.S. Al-Mutairi, A. N. Wilkinson, Addition of graphite filler to enhance electrical, morphological, thermal, and mechanical properties in poly (ethylene terephthalate): experimental characterization and material modeling, Polymers 11 (2019) 1411, https://doi.org/10.3390/polym11091411.
[45] K. Olszowska, M. Godzierz, S. Pusz, J. Myalski, A. Kobyliukh, G. Georgiev, A. Posmyk, B. Tsyntsarski, U. Szeluga, Development of epoxy composites with graphene nanoplatelets and micro-sized carbon foam: Morphology and thermal, mechanical and tribological properties, Tribol. Int. 185 (2023) 108556, https://doi.org/10.1016/j.triboint.2023.108556.
[46] C. Su, F. Lin, J. Jiang, H. Shao, N. Chen, Mechanical and electrical properties of graphene-coated polyimide yarns improved by nitrogen plasma pre-treatment, Text. Res. J. 91 (2021) 1627–1640, https://doi.org/10.1177/0040517520984102.
[47] B.A. Alshammari, M. Hossain, A.M. Alenad, A.G. Alharbi, B.M. AlOtaibi, Experimental and theoretical analysis of mechanical properties of graphite/polyethylene terephthalate nanocomposites, Polymers 14 (2022) 1718, https://doi.org/10.3390/polym14091718.
[48] L. Balea, G. Dusserre, G. Bernhart, Mechanical behaviour of plain-knit reinforced injected composites: effect of inlay yarns and fibre type, Compos Part B: Eng. 56 (2014) 20–29, https://doi.org/10.1016/j.compositesb.2013.07.028.
[49] A. Samanta, R. Bordes, Conductive textiles prepared by spray coating of water-based graphene dispersions, RSC Adv. 10 (2020) 2396–2403, https://doi.org/10.1039/C9RA09164E.
[50] C. Eid, E. Assaf, R. Habchi, P. Miele, M. Bechelany, Tunable properties of GO-doped $CoFe_2O_4$ nanofibers elaborated by electrospinning, RSC Adv. 5 (2015) 97849–97854, https://doi.org/10.1039/C5RA14897A.
[51] Y. Xu, T. Zhou, S. Huang, M. Xie, H. Li, H. Xu, J. Xia, H. Li, Preparation of magnetic Ag/AgCl/$CoFe_2O_4$ composites with high photocatalytic and antibacterial ability, RSC Adv. 5 (2015) 41475–41483, https://doi.org/10.1039/C5RA04410C.
[52] J. Qu, C. Qin, Y. Chen, F. Ding, Y. Zhang, G. Pan, X. Xu, X. Su, Activation of peroxymonosulfate by Co3Sn2 with Co(II)-enriched amorphous layer for efficient removal of RhB pollutant, Catal. Commun. 151 (2021) 106281, https://doi.org/10.1016/j.catcom.2021.106281.
[53] N.F. Attia, A.M. Eid, M.A. Soliman, M. Nagy, Exfoliation and decoration of graphene sheets with silver nanoparticles and their antibacterial properties, J. Polym. Environ. 26 (2018) 1072–1077, https://doi.org/10.1007/s10924-017-1014-5.
[54] M. Yousefi, M. Dadashpour, M. Hejazi, M. Hasanzadeh, B. Behnam, M. De La Guardia, N. Shadjou, A. Mokhtarzadeh, Anti-bacterial activity of graphene oxide as a new weapon nanomaterial to combat multidrug-resistance bacteria, Mater. Sci. Eng: C 74 (2017) 568–581, https://doi.org/10.1016/j.msec.2016.12.125.
[55] H. Zheng, R. Ma, M. Gao, X. Tian, Y.-Q. Li, L. Zeng, R. Li, Antibacterial applications of graphene oxides: structure-activity relationships, molecular initiating events and biosafety, Sci. Bull. 63 (2018) 133–142, https://doi.org/10.1016/j.scib.2017.12.012.
[56] S.U. Zaman, X. Tao, C. Cochrane, V. Koncar, Understanding the washing damage to textile ECG dry skin electrodes, embroidered and fabric-based; set up of equivalent laboratory tests, Sensors 20 (2020) 1272, https://doi.org/10.3390/s20051272.
[57] S. Rotzler, M. Schneider-Ramelow, Washability of E-textiles: failure modes and influences on washing reliability, Textiles 1 (2021) 37–54, https://doi.org/10.3390/textiles1010004.